Biomedical Engineering Letters (2019) 9:467–479
https://doi.org/10.1007/s13534-019-00130-y

ORIGINAL ARTICLE

A compact-sized surface EMG sensor for myoelectric hand prosthesis

Alok Prakash[1] · **Shiru Sharma**[1] · **Neeraj Sharma**[1]

Received: 17 April 2019 / Revised: 15 July 2019 / Accepted: 21 August 2019 / Published online: 26 August 2019

Abstract
Myoelectric prosthesis requires a sensor that can reliably capture surface electromyography (sEMG) signal from amputees for its controlled operation. The main problems with the presently available EMG devices are their extremely high cost, large response time, noise susceptibility, less amplitude sensitivity, and larger size. This paper proposes a compact and affordable EMG sensor for the prosthetic application. The sensor consists of an electrode interface, signal conditioning unit, and power supply unit all encased in a single package. The performance of dry electrodes employed in the skin interface was compared with the conventional Ag/AgCl electrodes, and the results were found satisfactory. The envelope detection technique in the sensor based on the tuned RC parameters enables the generation of smooth, faster, and repeatable EMG envelope irrespective of signal strength and subject variability. The output performance of the developed sensor was compared with commercial EMG sensor regarding signal-to-noise ratio, sensitivity, and response time. To perform this, EMG data with both devices were recorded for 10 subjects (3 amputees and 7 healthy subjects). The results showed 1.4 times greater SNR values and 45% higher sensitivity of the developed sensor than the commercial EMG sensor. Also, the proposed sensor was 57% faster than the commercial sensor in producing the output response. The sEMG sensor was further tested on amputees to control the operation of a self-designed 3D printed prosthetic hand. With proportional control scheme, the myoelectric hand setup was able to provide quicker and delicate grasping of objects as per the strength of the EMG signal.

Keywords Surface electromyography · Myoelectric prosthesis · Signal-to-noise ratio (SNR) · Control scheme · Grasp types

1 Introduction

Surface electromyography (sEMG) is a non-invasive technique for the assessment of the myoelectric signal. It is usually preferred because it is painless and quite easy to acquire [1]. The precise measurement and analysis of sEMG signals are utilized in various applications that include clinical diagnosis of neuromuscular disorders, the study of muscle fatigue, and control of prosthetics. Nowadays, sEMG has been established as a primary source of control for prosthetic hands due to their ease and intuitiveness [2–4]. A single-channel sEMG is sufficient to detect different activations of upper-limb muscles for numerous applications in rehabilitation and human–computer interface (HCI) [5].

Surface myoelectrodes give the basic assessment of the EMG signal under the skin. These are categorized into wet and dry type electrodes. Silver–silver chloride (Ag/AgCl) is a wet type electrode which provides good signal quality and low electrode–skin impedance, but have some limitations also. These electrodes may cause irritations and allergies to skin, and their long-time use can degrade the quality of the signal because gel in the electrode dries with time. Moreover, these require skin preparation, which increases the time and cost of measurement [6, 7]. These limitations make the wet electrodes unsuitable for the prosthetic application. Dry electrodes, on the other hand, do not require gel as well as skin preparation procedure reducing time and effort to set up. Although these electrodes may have higher skin–electrode impedance and susceptible to motion artifacts, however, there is a possibility of getting stronger sEMG signal with these electrodes [8]. Laferriere et al. [9] proposed dry flexible electrodes and compared its performance with the commercial Ag/AgCl electrodes for detecting muscle contractions under different loading conditions. A finely machined toothed silver electrode was developed for acquiring EMG signal, which showed performances similar to gelled type electrode and better than flat silver surface [10].

✉ Alok Prakash
alokp.rs.bme15@itbhu.ac.in

[1] School of Biomedical Engineering, Indian Institute of Technology (BHU), Varanasi 221005, India

The myoelectric prosthesis mainly consists of a device for capturing EMG signal, a controller for processing these signals and generating a control command in real-time to drive actuator mechanically linked with the prosthetics [11, 12]. The operation of smart EMG based prosthesis, working as an artificial substitute to missing limbs, is affected by numerous factors like change in position of the electrode, variation in the level of muscle contraction, the positioning of the forearm and limb orientation [13].

A control scheme in myoelectric prosthesis translates the information contained in the EMG signal to control command for actuation of prosthetic devices. The proportional scheme is a non-pattern recognition based myoelectric control scheme in which the speed and force of the prosthetic hand is controlled using the intensity of the EMG signal in a proportional manner [14, 15]. Such a scheme relies on factors like characteristics of EMG sensor, data acquisition system, sensor position on the skin, physiology of muscles, and muscle fatigue for proper generation of control commands [16, 17].

The most common noise sources interacting with the EMG signals are inherent noise, motion artifacts, electromagnetic noise, and crosstalk [18–20]. For correct recognition of EMG signal patterns, the sensor typically consists of electrodes and signal conditioning unit. Noise removal, signal boosting, and signal translation are the key tasks performed by the signal conditioning section present in the EMG system. Moreover, the quality of the myoelectric signal for operation of prosthetics largely depends on the signal conditioning circuitry of the EMG detection unit [21]. The quality of the EMG signal can be evaluated by the estimation of signal-to-noise (SNR) values through automatic or manual detection of myoelectric bursts and baseline noise from the signal in the time domain [22].

Modern EMG systems with a large number of features offer a high-quality recording of myoelectric signals. However, the main issues with all these commercial EMG systems are their extremely high cost, non-portability, complexity, and inability to provide an open source platform [23, 24]. Clinical diagnostics requires high-end EMG equipment capable of giving high quality and multichannel signals. Such devices mainly target offline data analysis. Hence, there is no bar on their response time [25]. Whereas for prosthetic control, moderate quality EMG device with less response time (below 300 ms) and a high degree of intuitiveness are required [26, 27]. Also, the device should be simple, affordable, and compact enough to fit inside the prosthetic hand socket [28]. Table 1 describes the technical specifications and cost of some commercially available EMG devices [29–31].

In the proposed work, a compact-sized sEMG sensor has been developed for the upper limb prosthetic application. The high sensitivity and increased SNR feature of the sensor allow faithful detection of weaker strength sEMG signal, particularly from amputees. These parameters of the sensor, along with its lower (fast) response time, offers the smooth and faster operation of the prosthetic device. The sensor produces a smooth linear envelope output of 0–5 V, which is proportional to the intensity of the EMG signal. Section 2 describes the materials and methods of the designed sEMG sensor. Section 3 deals with the experimental setup for the assessment of sensor performance. Results and discussion are provided in Sect. 4. Section 5 describes the application of developed EMG sensor for prosthetic hand control. Finally, the conclusion is given in Sect. 6.

2 Materials and methods

2.1 Design and construction of the sensor

The proposed sEMG sensor mainly consists of silver palette electrodes as an electrode interface, a signal conditioning section, and a power supply unit all embedded in a single structure. Figure 1a shows the block diagram of the proposed sEMG sensor.

Table 1 Technical features of available EMG sensors

	Ottobock 13E200	Myo armband	Myoware muscle sensor
Input	7.4 V	3.7 V	5 V
Output type	0–5 V envelope	Differential (±2.5 mV)	0–5 V envelope, differential (±2.5 V)
Type of electrodes	Stainless steel	Stainless steel	Disposable Ag/AgCl
Number of channels	1	8	1
Power supply	External	Integrated	External
Weight	4.5 g	93 g	9 g
Output accessibility	Easily accessible	Does not provide open source platform	Easily accessible
Price	$400	$200	$37.95

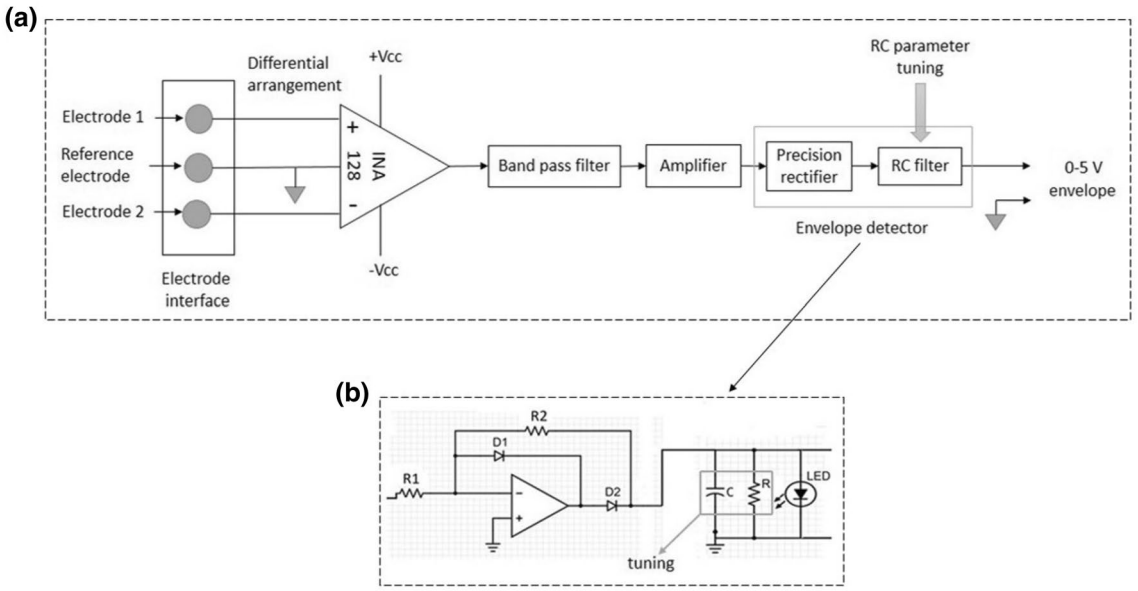

Fig. 1 **a** Block diagram representation of the proposed EMG sensor, **b** detailed circuit for the envelope detector

2.1.1 Design of skin interface

The skin interface of the sensor was designed using three silver palette electrodes of 1.24 cm diameter each. All the electrodes were embedded in the sensor base at an inter-electrode distance of 1.25 cm, which is shown in the Fig. 3a. The two electrodes at the end position are intended for target muscles while the middle electrode serves as a reference to make the whole arrangement a differential one. This configuration of electrodes minimizes the motion artifacts which occurs due to the movement of electrode cables [32]. Silver metal as a surface myoelectrode serve several advantages such as the good property of biosignal conduction as well as biocompatibility, does not require skin preparation, works well under sweat and wet conditions, cheaper for long-term use, non-toxic and non-reactive, etc. [8–10].

2.1.2 Design of signal conditioning circuitry

A signal conditioning circuitry consisting preamplifier, a band-pass filter, inverting amplifier and envelope detector, was designed for converting the raw sEMG signal directly from the electrodes to an even voltage signal. Figure 1a describes the different stages involved in the EMG signal conditioning unit.

In the pre-amplification stage, an instrumentation amplifier (i.e., INA 128P IC) was employed which offers benefits like high common-mode rejection ratio (CMRR), low offset voltage, low power consumption, and adjustable gain. To prevent the saturation and instability of subsequent amplifier stages, a gain of this stage adjusted to a lower value of 11.4 [33].

A band-pass filter has been added with a lower cut-off frequency of 11.4 Hz and the higher cut-off frequency of 323.7 Hz. This stage was implemented to remove the motion artifacts and external noises of low frequencies and noises occurring at high frequencies. The band pass filter circuit was realized with a gain of 2.92 to increase the voltage level of the filtered signal. The overall transfer function of the designed band-pass filter is described in Eq. (1).

$$G(s) = \frac{12{,}181{,}527.9s^2}{\left(s^2 + 166.661s + 5201.05\right)\left(s^2 + 4837.01s + 4{,}137{,}219.2181\right)}. \tag{1}$$

The second stage of amplification was done at a gain of 109.7 to increase the amplitude of the EMG signal to a level such that it can be easily accessed by storage as well as control devices. The overall gain achieved until this stage was 3700.

An envelope detector circuit comprising a precision rectifier circuit and low pass RC circuit shown in Fig. 1b, was implemented to produce a linear envelope of amplified and filtered EMG signal [34]. This stage was realized such that the amplitude of the EMG signal remains unaffected by other factors except for muscle excitation [35]. The time constant of the RC filter should be ranged from 10 to 150 ms to produce a clear envelope of EMG signal [36, 37]. Charging and discharging time constant of the RC filter circuit mainly regulates the rise and fall time as well as the shape of the generated envelope [38]. The value of R and C was tuned manually to achieve a time constant of 110 ms, which leads

to the generation of the smooth and faster envelope with less rise time and sufficient fall time, intended for prosthetic application. The output of this stage is a linear envelope of 0–5 V, which is proportional to the strength of muscle contraction. An LED connected across the final output of the envelope detector indicates the production of EMG signal in terms of its glowing intensity.

2.1.3 Power supply unit

Power supply unit in the sensor includes: (1) a rechargeable lithium-polymer battery of 3.7 V, 240 mAh capacity (2) a step-up chopper (3) unipolar to bipolar supply circuit. Figure 2 shows the block diagram and the detailed circuitry for the incorporated power supply unit. MT3608 step-up converter module (from Aerosemi) has been utilized as a step-up chopper in the power supply unit. It mainly includes a power MOSFET which receives fixed switching frequency from automatic pulse frequency modulation. The chopper circuit with adjustable gain increases the amplitude level of dc voltage from the battery (i.e., 3.7–12 V). To power, the active components present in the signal conditioning circuitry, a specific circuit shown in Fig. 2b was incorporated which converts the unipolar voltage from the chopper to bipolar supply (i.e., 12 V to ±6 V). The integration of the power supply unit within the sensor module eliminates the requirement of an external dual power source which can make the acquisition setup complex and bulky.

2.1.4 Sensor description

Figure 3a depicts the rear view of the sensor, i.e., sensor base showing the electrode interface whereas Fig. 3b describes the front view of the sensor comprising the signal conditioning circuitry and power supply unit. The dimension of the developed sensor is 25×70 mm^2, which can be further reduced (up to one-third of the original dimension) by using small size SMD (surface-mount devices) components and professional tools for fabrication. The power consumption of the developed sensor was estimated 30 mA using the datasheets of the components employed in the circuitry.

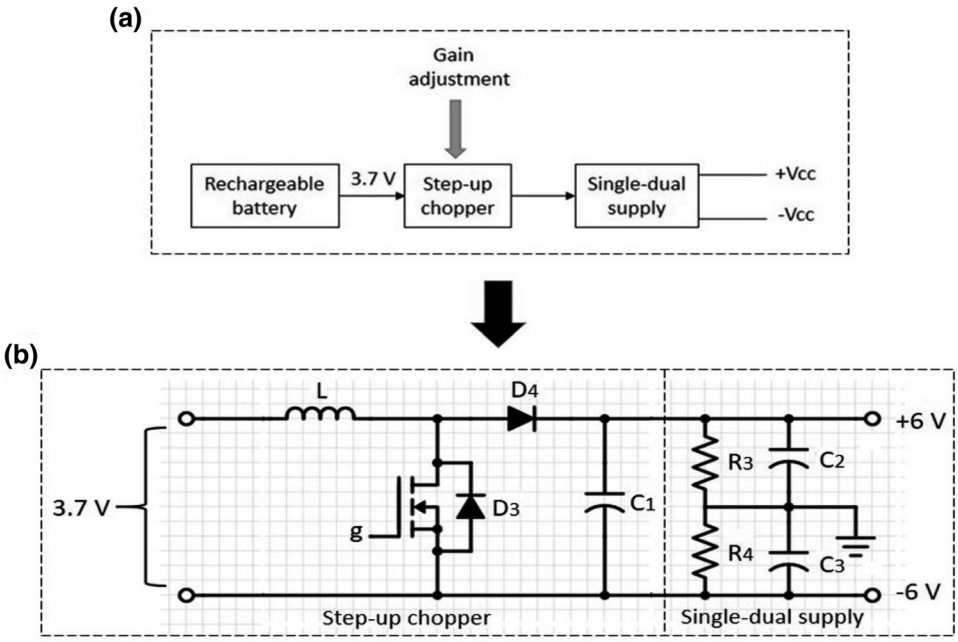

Fig. 2 **a** Block diagram of the power supply unit, **b** detailed circuitry for the power supply unit

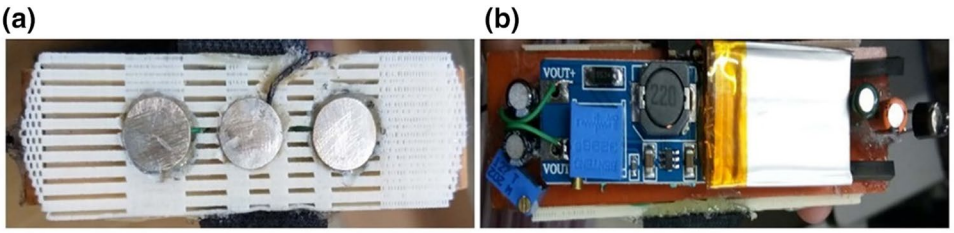

Fig. 3 **a** Rear view of the developed sensor, **b** front view of the developed sensor

3 Experimental setup for assessment of sensor performance

3.1 Selection of sensor for comparison

In order to validate the performance of the developed sEMG sensor, its output characteristics were compared with the commercial EMG sensor. Referring to Table 1, it was observed that Ottobock 13E200 and myoware muscle sensor are the two devices which provide similar kind of output as the developed sensor (i.e., linear envelope). Out of these two devices, myoware muscle sensor was selected for comparison because of its low cost, easy availability, and decent performance in prosthetics [2]. EMG data were acquired from a total of 10 subjects (3 amputees and 7 intact) using both the sensors for determining their output parameters. Ethical approval was taken from the Ethical committee, Institute of medical sciences, BHU, Varanasi before performing this experiment. Details of each amputee participated in this work with their type, and the reason for amputation are described in Table 2.

Table 2 Details of amputees participated in EMG data acquisition

S. no.	Gender	Age	Weight (kg)	Type of amputation	Reason of amputation
1.	Male	20	50	Transradial (left hand)	Accident
2.	Male	50	85	Transradial (right hand)	Accident
3.	Male	12	25	Transradial (right hand)	Accident

3.2 Positioning of sensors

For acquiring the EMG data, both the sensors were attached to the forearm muscles of subjects as shown in the Fig. 4. As the developed sensor is dry electrode based, it was attached using velcro tape, whereas the myoware muscle sensor was fixed through disposable Ag/AgCl electrodes. The target electrodes of both the sensors were placed at flexor carpi radialis and flexor carpi ulnaris while the reference electrode of the myoware sensor was placed at the elbow portion. These specified muscle groups on the forearm are directly responsible for the palm and wrist movements of interest [23].

3.3 Defining the level of muscular contraction

The EMG data for all the subjects were recorded for a different level of contractions (i.e., contractile force) of their forearm muscles. As the amputees cannot perform natural hand activities with their residual limb, therefore, to maintain uniformity in EMG data, same activities were decided for amputees as well as healthy subjects. The different levels of contractile force were selected from the force exerted by

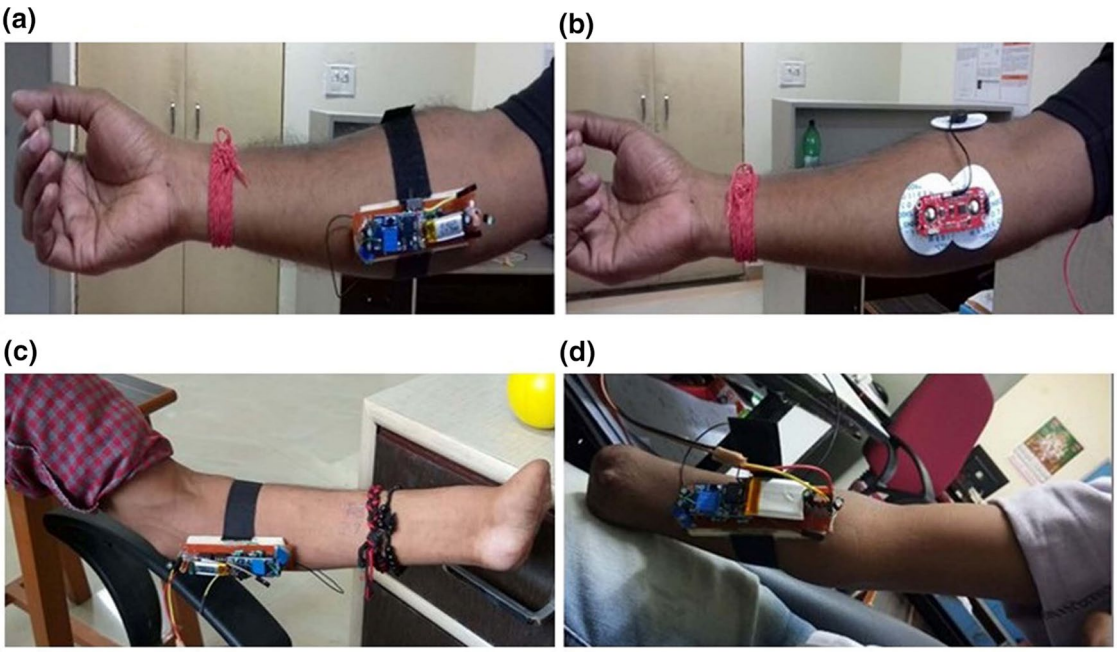

Fig. 4 Attachment of both the sensors on different subjects

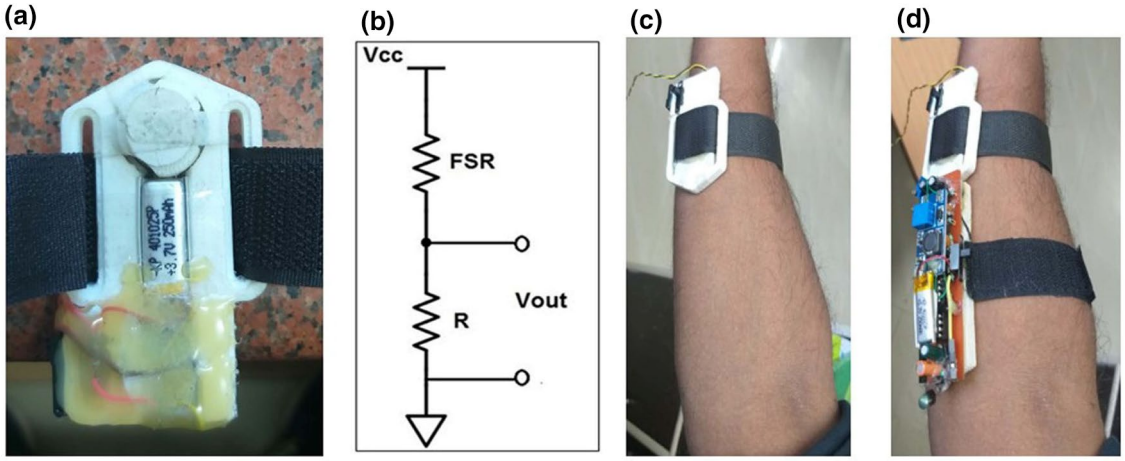

Fig. 5 **a** Sensing area of the FSR band, **b** output circuit for the band, **c** attachment of band to the forearm, **d** attachment of the developed sensor and band together to the forearm

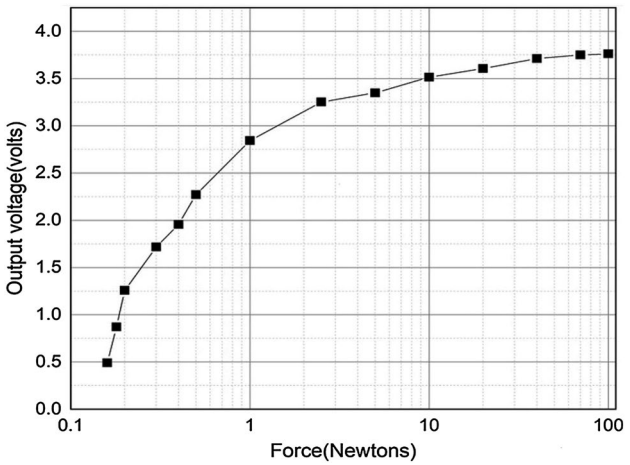

Fig. 6 Force voltage calibration curve for FSR band

flexor muscles on the force sensitive resistor (FSR) during contraction. A highly sensitive band comprising FSR was developed for the measurement of muscular contractile force in terms of voltage. The FSR sensing portion was encased in a 3D printed structure for proper distribution of muscular contractile force over the contact surface area. Figure 5 shows the sensing area of the designed FSR band, its voltage divider circuit for converting the change in resistance of FSR to voltage output and its attachment to the forearm for measuring contractile force. Using the force curve from the FSR datasheet (FSR 406) and circuit in the Fig. 5b, a force voltage calibration curve was obtained, which is shown in Fig. 6 [39]. From the obtained calibration curve, a maximum of six different levels of muscular contractions was defined for recording EMG data, which are indicated in Table 3. The output voltage of the 6th level corresponds to the maximum

Table 3 Allocation of different levels of muscular contractions

FSR output voltage (V)	Force (N)	Contraction level
0.8	0.18	1
1.25	0.2	2
1.7	0.3	3
2.2	0.5	4
2.8	1	5
3.2	2.5	6

voluntary contraction (MVC) of the forearm muscle. Attachment of developed sensor and FSR band was done together on the forearm muscles as shown in Fig. 5d for recording EMG signal at different contraction levels.

3.4 Data acquisition

EMG data acquisition was performed using NI ELVIS II$^+$ hardware and Lab VIEW 2015 software interface. As per the levels defined in Table 3, the subjects were asked to perform 6 different levels of muscular contractions of their forearm, and 10 repeated readings were recorded for each level. Duration of each reading was 6 s. All the data were acquired at a sampling rate of 2 kS/s.

4 Results and discussion

The developed EMG sensor mainly depends on the performance of the electrode interface as well as the employed signal conditioning circuitry. There are several measures used to quantify the quality of electrodes. The most prominent

are electrode–skin contact impedance and signal-to-noise ratio (SNR) [40].

Similarly, the overall output performance of the developed sensor can be analyzed by various characteristics like SNR, amplitude sensitivity, and response time. Therefore the performance parameters of the proposed electrode and the sensor were separately determined and compared with that of the standard system.

4.1 Electrode performance

The performance of silver palette electrodes embedded in the sensor was compared with the standard disposable Ag/AgCl electrodes regarding electrode–skin impedance and signal-to-noise ratio (SNR).

4.1.1 Electrode–skin impedance

Grimnes's method was used for determining the electrode–skin impedance of individual surface electrode [41]. A constant sinusoidal current of 50 μA at 50 Hz (generated by a voltage controlled current source) was passed through the skin from one electrode and exited from the other. The impedance values for the proposed electrodes and disposable electrodes were obtained and recorded using Lab VIEW with NI ELVIS II$^+$ hardware interface at a sampling frequency of 2 kS/s. The location of both the electrodes was kept the same for measurement of each impedance. Impedance versus time plot for both the electrodes was obtained using the recorded data for 15 min. The impedance values for the proposed electrode showed a decrease over time, which is quite clear from Fig. 7. In general, the lower impedance is desired for better conduction of electrodes [40]. A comparison regarding observed impedance values for both electrodes is provided in Table 4. After a certain settling time, dry metal electrodes show comparable impedance values to that of wet type electrodes [8].

4.1.2 Electrode SNR

Assessment of noise performance of the proposed electrode was analyzed through evaluation of signal-to-noise ratio (SNR). SNR was determined as the ratio of root mean square (RMS) value of raw EMG signal recorded during muscular contraction to the RMS value of the undesired signal (i.e., baseline noise) recorded while the muscle is at rest [22]. The raw EMG signals with both the electrodes were recorded for maximum voluntary contraction (MVC) of the forearm muscle, whereas the undesired signals were recorded for no contraction. The data of 6 s duration were acquired for each subject. Using Eq. (2), the SNR value was evaluated for each subject. Average SNR values of all the subjects determined for both the electrodes are mentioned in Table 4. The result

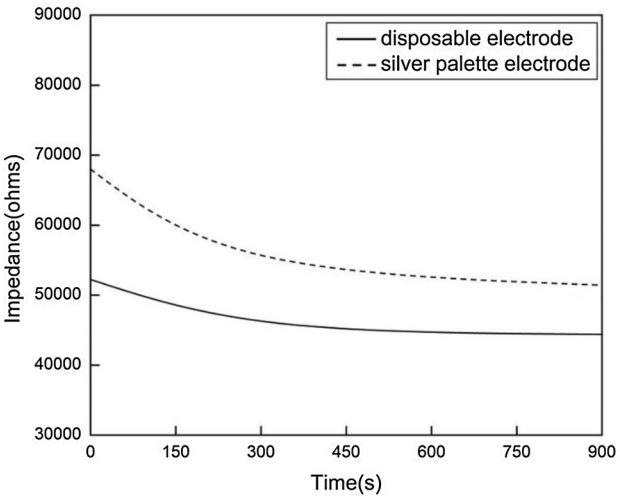

Fig. 7 Obtained impedance response for both the surface electrodes

Table 4 Performance comparison for surface electrodes

S. no.	Type of electrode	Area (mm^2)	Impedance (kΩ)	SNR (dB)
1	Disposable Ag/AgCl	314	48	24.4
2	Silver palette	120	59	26.7

in the table shows that the proposed electrode provides similar SNR values as the conventional Ag/AgCl electrode.

$$\mathrm{SNR} = 20\log_{10}\left(\frac{\mathrm{RMS}_{\mathrm{signal}}}{\mathrm{RMS}_{\mathrm{noise}}}\right) \quad (2)$$

4.2 Sensor performance

4.2.1 Output

Figure 8 shows the EMG signals for 6 different levels of muscular contractions (i.e., activities) of an amputee recorded with both the sensors. To quantitatively analyze the similarity between the signals of both the sensors a two-tailed paired t-test was conducted. The similarity test was performed using EMG data of all the 10 subjects considering their every level of muscular contraction separately. The result showed high Pearson's correlation coefficient ($r > 0.95$) with p value < 0.0001, revealing the pairing were significantly effective.

4.2.2 SNR

To analyze the signal quality of both the sensors, their SNR values were determined. EMG signals using both

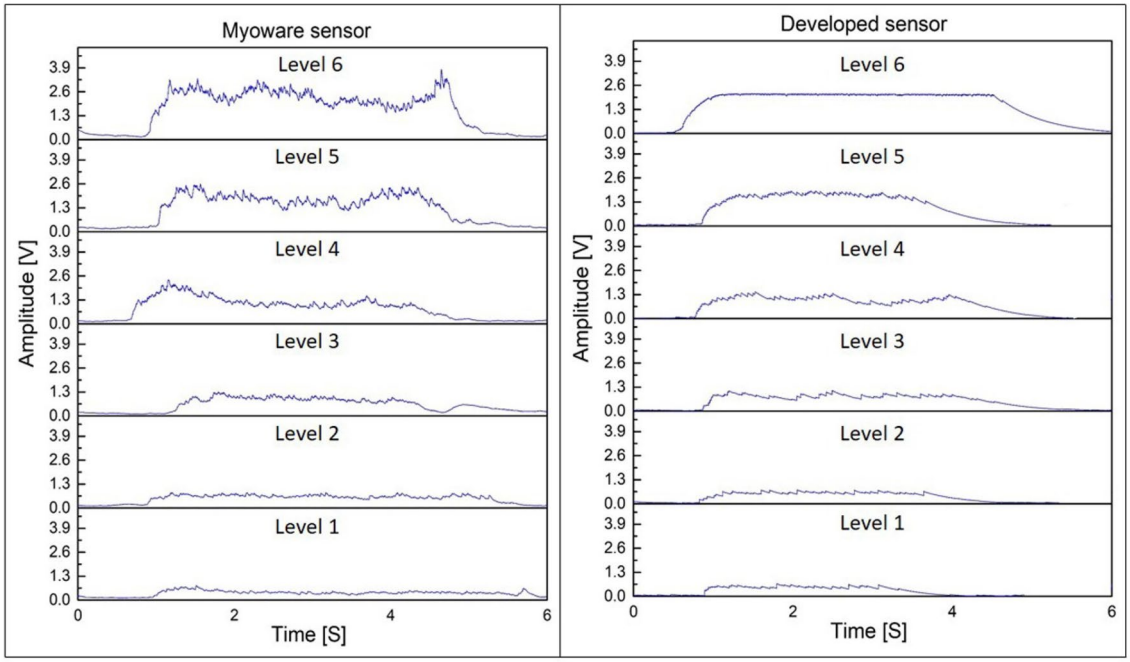

Fig. 8 Envelopes produced by the two sensors for six different levels of muscular contractions of an amputee

the sensors were acquired for the same contractile force of forearm muscle (i.e., for MVC) while noises were acquired for no contraction. Figure 9a shows an EMG waveform indicating baseline noise and signal strength, whereas Fig. 9b, c describes the recorded baseline noises for a subject with both the sensors. For each subject, SNR value was calculated using Eq. (2) considering data of 6 s duration. Table 5 gives the evaluated SNR values for all the subjects with both the sensors. In the results, higher SNR values were observed for the developed sensor as compared to the commercial sensor. SNR measures the quality of the EMG signal and can range between 10 and 50 dB under ideal, simulated situations [42].

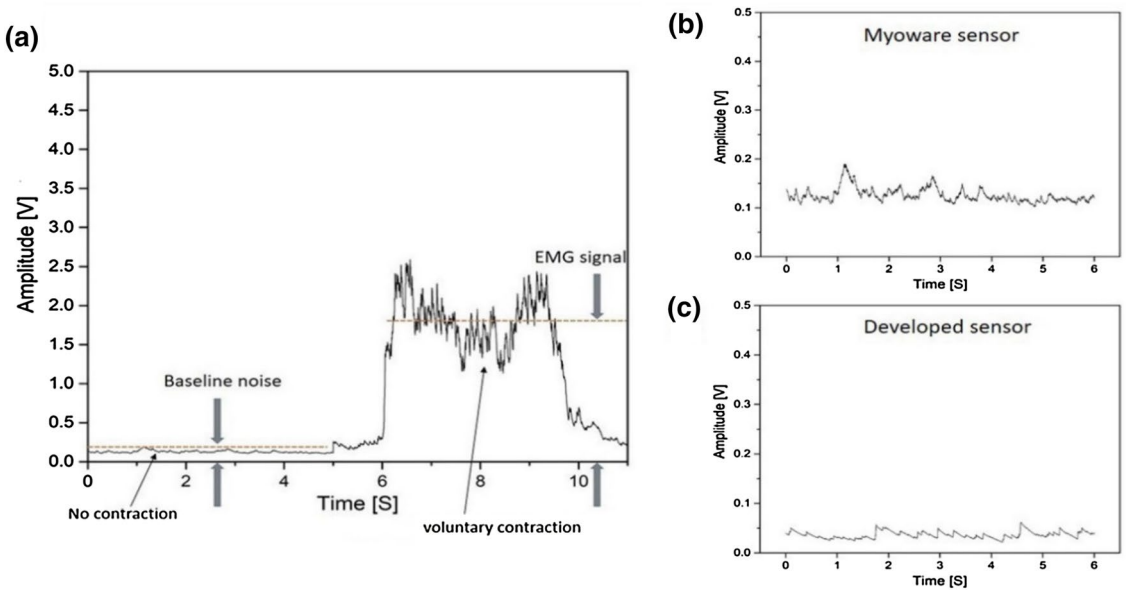

Fig. 9 **a** SNR calculation from recorded EMG envelope, **b** baseline noise for myoware sensor, **c** baseline noise for developed sensor

Table 5 Evaluated SNR by sensor type

Subject	Sensor	SNR (dB)
1	Developed	32.86
	Myoware	24.08
2	Developed	32.46
	Myoware	23.32
3	Developed	32.66
	Myoware	22.92
4	Developed	32.86
	Myoware	23.52
5	Developed	33.02
	Myoware	22.49
6	Developed	32.78
	Myoware	23.20
7	Developed	33.06
	Myoware	23.86
8	Developed	33.25
	Myoware	23.36
9	Developed	33.17
	Myoware	23.93
10	Developed	33.47
	Myoware	23.24
Average value	Developed	32.95
	Myoware	23.39

4.2.3 Sensitivity

Sensitivity analysis was performed for both the sensors to test the ability of the developed sensor module in detecting EMG amplitude variations from various subjects. Amplitude sensitivity for the sensors was evaluated as the ratio of incremental change in the EMG output voltage to the change in the muscular contractile force (i.e., input to the EMG sensor) [43, 44]. A plot was obtained for a corresponding change of average EMG voltage (for subjects) with a change in muscle contractile force for both the sensors. The slope of the obtained linear curve was calculated to give the sensitivity of the sensor. Figure 10a, b shows the sensitivities of both the sensors for all the subjects and only amputees. The results showed that the developed sensor was 45% more sensitive than the myoware sensor in detecting signal from all the subjects whereas in the case for only amputees it was 70% more sensitive than the myoware muscle sensor. Sensitivities of both the sensors were determined at a fixed gain value at which their SNR is maximum. Because as we increase the gain of an EMG system above a certain value, its baseline noise increases, which decrease the SNR value of the system [22].

4.2.4 Response time

The response time of the sensor was evaluated in terms of rise and fall time of its output envelope. Rise time was measured as the time required for the envelope to rise from 10 to 90% of its largest value. Conversely, fall time was calculated as the time taken by the envelope to fall from 90 to 10% of its maximum value [45]. Figure 11 shows the estimation of rise and fall time from the produced EMG envelope. Rise and fall time was computed from the EMG envelopes generated with both the sensors placed at the same muscle group for similar contractile force. For each subject, response times were determined for all the 6 levels of muscular contractions (defined in Table 3) using both sensors.

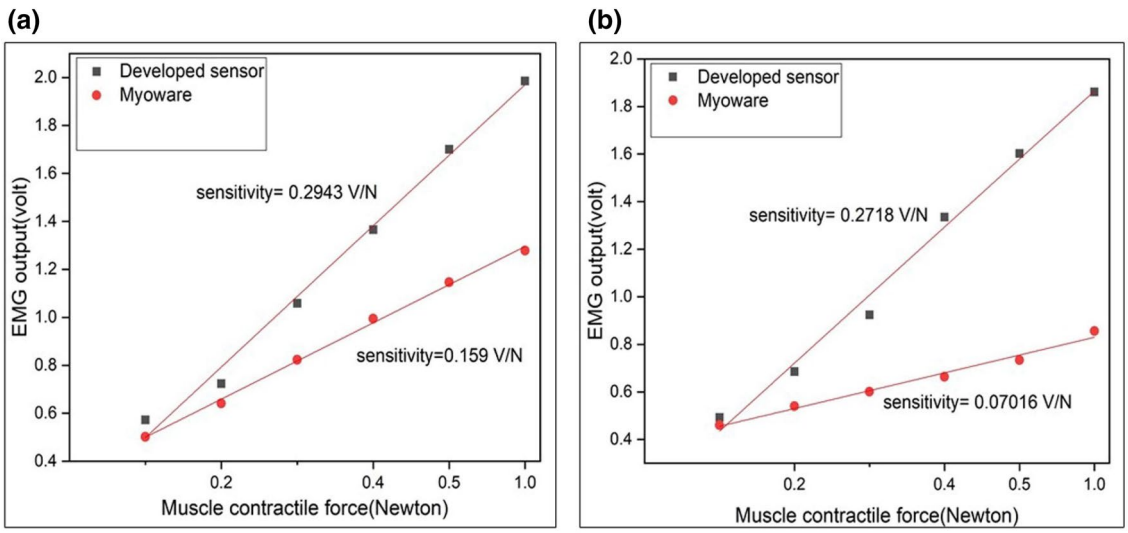

Fig. 10 **a** Sensitivities of sensors for all the subjects, **b** sensitivities of sensors for only amputees

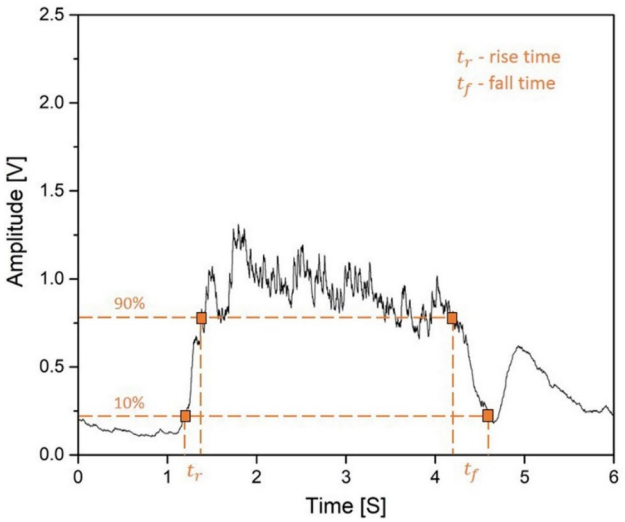

Fig. 11 Rise and fall time calculation from an EMG envelope

Table 6 Rise and fall time for both the sensors

Muscular contraction level	Rise time, t_r (ms)		Fall time, t_f (ms)	
	Myoware	Developed sensor	Myoware	Developed sensor
1	260	110	190	300
2	280	110	220	360
3	310	130	230	390
4	340	140	270	430
5	370	160	310	480
6	380	170	350	490
Average	323	136	261	408

In Table 6, the first six rows indicate the average rise and fall time calculated for each contraction level considering all the subjects while the last row gives the overall rise and fall time for the sensors. The rise time for the developed sensor was obtained to be 57% faster (lower) than the myoware sensor whereas the fall time for the sensor was observed 36% higher in comparison to the commercial sensor. Since the myoelectric control signal has a delay time of about 300 ms from the time when user intention is given, the rise time of the developed sensor is better and suitable for the intuitive application [17, 27, 46].

5 Sensor utilization for prosthetic hand control

The developed sensor was further utilized to control the operation of a 3D printed prosthetic hand by capturing the EMG signal from amputees. For this, a 3D printed hand prototype was prepared and was intrinsically actuated using two high torque servomotors (MG-995) [47]. Fingers were equipped with silicon fingertip for improving the grasping capability of the hand. A microcontroller chip (Arduino Nano) was installed inside the hand which receives analog input from the EMG sensor and provides a digital output to servomotors. All the electrical, as well as electronic components present within the hand, were powered using 2000 mAh, lithium-ion battery.

The proportional control strategy was implemented in the microcontroller section, which translates the EMG signal from the sensor to PWM output for driving servomotor. This strategy provides proportional actuation of the prosthetic hand fingers as per the intensity of the EMG signal, i.e., larger strength of EMG signal corresponds to the greater grasping force of fingers to close the hand. Figure 12 shows the scheme for the generation of control commands for real-time operation of the 3D printed prosthetic hand.

The sEMG sensor was attached on the residual forearm stump of amputees as shown in Fig. 3 for real-time control of the designed prosthetic hand. The amputees were able to dexterously grasp different shaped objects with the hand using their muscular contractions (i.e., the intensity of EMG signal). Figure 13 shows the grasping of various objects with the prosthetic hand, using EMG signals from an amputee.

The proportional myoelectric control provides the operating speed of the prosthetic hand that is dependent on the intensity of the EMG signal. This feature enables intuitive control and faster-grasping capability to the hand [14, 15, 48]. The operation speed of the myoelectric hand setup was analyzed in terms of its response time. An experiment was performed in which response time (i.e., Closing/opening

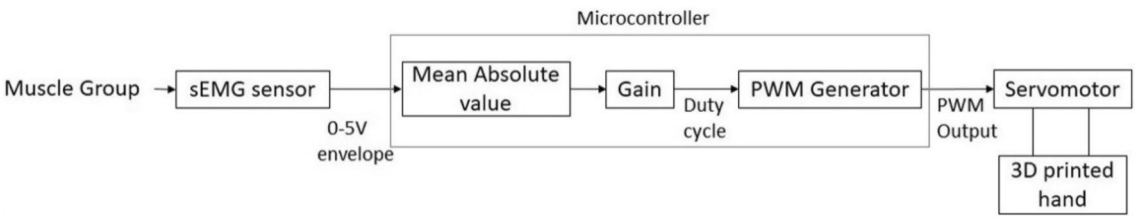

Fig. 12 Generation of control command using EMG signal from the sensor

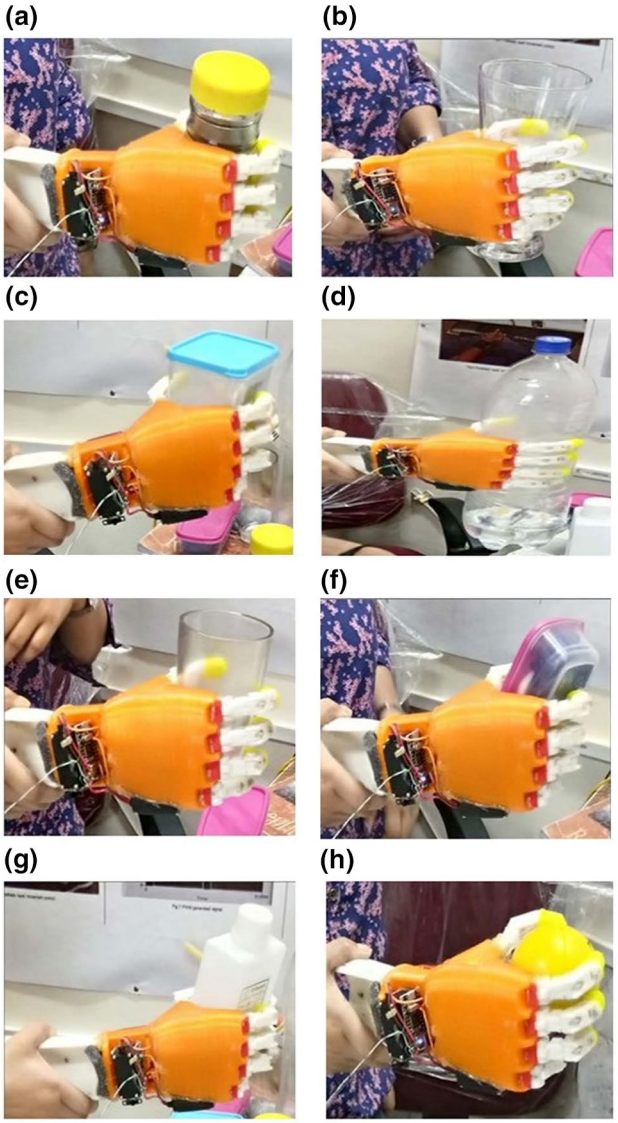

Fig. 13 Grasping of various objects performed by prosthetic hand using EMG signals from an amputee

time) of the prosthetic hand with both the sensors was determined from their recorded video of hand operation. The full closing and full opening time of prosthetic hand fingers with both the sensors are provided in Table 7. Faster closing and slower opening operation of the prosthetic hand was observed with the developed sensor as compared to the myoware sensor. Based on the survey report of amputees, researchers recommended 300–400 ms as the acceptable closing time for the myoelectric prosthesis [27, 46, 49].

The operating speed of the prosthetic hand is primarily regulated by the combined effect of EMG sensor delay, microcontroller processing time, and the response time of the servomotor. Processing time of the Arduino nano microcontroller (in generating control command) and response time of the servomotor (MG-995) as per their datasheets are

Table 7 Response time of hand with both the sensors

Prosthetic hand	Full closing time (ms)	Full opening time (ms)
With developed sensor	350	650
With myoware muscle sensor	550	450

40 ms and 160 ms [27]. Therefore, analyzing Tables 6 and 7 it can be concluded that the closing time of the hand mainly depends on the rise time of the EMG sensor envelope and conversely the opening time depends on the fall time of the envelope.

6 Conclusion

In this paper, a dry electrode based sEMG sensor has been designed for upper limb prosthetic application. The compact structure of the sensor makes it wearable for a long time used inside the prosthetic hand socket. The Silver palette electrodes used in the sensor showed decent performance, i.e., electrode–skin impedance and SNR values as compared to the standard Ag/AgCl electrodes.

The developed sensor showed better output parameters such as SNR, sensitivity, and response time as compared to the commercial sensor. Comparison of full features between both the sensors is provided in Table 8.

The sensor was successfully tested on amputees for the real-time controlled operation of the developed prosthetic hand. Implementation of a proportional control scheme enables the grasping force of the hand fingers proportional to the EMG signal strength. Amputees based on their EMG signal intensity were able to grasp different shaped objects with the hand.

The higher sensitivity with greater SNR values of the developed sensor facilitates reliable detection of sEMG signal from subjects (particularly amputees) and yield smoother operation of the prosthetic device. The operating speed (i.e., closing/opening time) of the prosthetic hand is highly influenced by response time (i.e., rise and fall time) of the sensor. The lower (faster) rise time of the sensor offers faster closing of the prosthetic hand fingers to grasp the objects (when the muscle is activated) whereas higher fall time provides some delay in the opening of hand fingers to prevent the immediate release of grasped objects (when the muscle is instantly relaxed). The tuning of RC parameters in the envelope detection stage of the sensor was mainly responsible for the generation of a smoother envelope with lower rise time and higher fall time. The developed EMG sensor implemented with proportional control strategy was able to

Table 8 Comparison of the developed sensor with commercial myoware sensor

Features	Myoware muscle sensor	Developed EMG sensor
Output type	0–5 V EMG envelope	0–5 V EMG envelope
Electrode type	Disposable Ag/AgCl	Silver palette
Inter-electrode distance	4 cm	1.25 cm
Power supply unit	External	Integrated
Power consumption	9 mA	30 mA
Mass	9 g	42 g
Dimension	20×52 mm^2	25×70 mm^2
SNR	23.39 dB	32.95 dB
Sensitivity	0.159 V/N	0.2943 V/N
Rise time	323 ms	136 ms
Fall time	261 ms	408 ms
Price in the commercial market	$37.95	Prototyping cost ($13)

provide smooth and faster operation of a prosthetic hand with control on grasp force.

The dry electrodes integrated in the skin interface of the sensor offers several benefits over the conventional Ag/AgCl electrodes such as cheap for longer-time use, does not require any skin preparation, does not causes allergies and skin irritation when used for longer duration, signal quality remains consistent over time, good performance under sweat and wet conditions etc. Also, the presence of power supply within the sensor eradicate the need for external bipolar supply, which can create a complexity to the acquisition setup. The power consumption of the developed sensor is higher than the myoware sensor however with a rechargeable battery of 350 mAh it can last up to 11 h of continuous use. Larger mass and dimension are some demerits of the designed sensor which can be overcome by using tiny sized SMD components and specialized tools for fabrication.

In future work, the EMG signals acquired with the sensor for different muscular contraction levels can be easily classified to achieve individual finger movement of the prosthetic hand. This will enhance the number of grip patterns for a more precise and natural grasping of objects. Also, such a simple, effective, and low-cost sensor can be deliberately utilized in the development of the affordable myoelectric hand.

Acknowledgements The authors would like to thank the Design Innovation Centre, Indian Institute of Technology (BHU) for funding this project.

Funding This research work was funded by Design Innovation Centre, Indian Institute of Technology (BHU).

Compliance with ethical standards

Conflict of interest The authors declare that there are no conflicts of interest.

Ethical approval (involvement of animals) This article does not contain any studies with animals performed by any of the authors.

Ethical approval (involvement of human subjects) This article involves surface EMG data acquisition from various human subjects. Ethical approval was taken from the Ethical committee, Institute of medical sciences, BHU, Varanasi before performing this experiment. All procedures performed in studies involving human participants were in accordance with the ethical standards of the institutional and/or national research committee and with the 1964 Helsinki declaration and its later amendments or comparable ethical standards.

Informed consent Informed consent was obtained from all individual participants included in the study.

References

1. Day S. Important factors in surface EMG measurement. Calgary: Bortec Biomedical Ltd Publishers; 2002. p. 1–7.
2. Tavakoli M, Benussi C, Lourenco JL. Single channel surface EMG control of advanced prosthetic hands. Expert Syst Appl. 2017;79:322–32.
3. Liu J, Zhou P. A novel myoelectric pattern recognition strategy for hand function restoration after incomplete cervical spinal cord injury. IEEE Trans Neural Syst Rehabil Eng. 2013;21:96–103.
4. Pancholi S, Joshi AM. Portable EMG data acquisition module for upper limb prosthesis application. IEEE Sens J. 2018;18:3436–43.
5. Phinyomark A, Phukpattaranont P, Limsakul C. Fractal analysis features for weak and single-channel upper-limb EMG signals. Expert Syst Appl. 2012;39:11156–63.
6. Baek J-Y, An J-H, Choi J-M, Park K-S, Lee S-H. Flexible polymeric dry electrodes for the long-term monitoring of ECG. Sens Actuators A. 2008;143:423–9.
7. Pylatiuk C, Muller-Riederer M, Kargov A, Schulz S, Schill O, Reischl M, et al. Comparison of surface EMG monitoring electrodes for long-term use in rehabilitation device control. In: 2009 IEEE international conference on rehabilitation robotics [Internet]. Kyoto, Japan: IEEE; 2009 [cited 2018 Dec 3]. p. 300–4.
8. Searle A, Kirkup L. A direct comparison of wet, dry and insulating bioelectric recording electrodes. Physiol Meas. 2000;21:271.
9. Laferriere P, Lemaire ED, Chan ADC. Surface electromyographic signals using dry electrodes. IEEE Trans Instrum Meas. 2011;60:3259–68.
10. Jamal MZ, Kim K-S. A finely machined toothed silver electrode surface for improved acquisition of EMG signals. In: 2018 IEEE

Sensors Applications Symposium (SAS) [Internet]. Seoul: IEEE; 2018 [cited 2018 Dec 3]. p. 1–5.
11. Parker P, Englehart K, Hudgins B. Myoelectric signal processing for control of powered limb prostheses. J Electromyogr Kinesiol. 2006;16:541–8.
12. Asghari Oskoei M, Hu H. Myoelectric control systems—a survey. Biomed Signal Process Control. 2007;2:275–94.
13. Khushaba RN, Al-Timemy A, Kodagoda S, Nazarpour K. Combined influence of forearm orientation and muscular contraction on EMG pattern recognition. Expert Syst Appl. 2016;61:154–61.
14. Lenzi T, De Rossi SMM, Vitiello N, Carrozza MC. Proportional EMG control for upper-limb powered exoskeletons. In: 2011 annual international conference of the IEEE Engineering in Medicine and Biology Society [Internet]. Boston: IEEE; 2011 [cited 2018 Dec 3]. p. 628–31.
15. Fougner A, Stavdahl O, Kyberd PJ, Losier YG, Parker PA. Control of upper limb prostheses: terminology and proportional myoelectric control—a review. IEEE Trans Neural Syst Rehabil Eng. 2012;20:663–77.
16. Herle S, Man S, Lazea G, Raica P. Myoelectric control strategies for a human upper limb prosthesis. J Control Eng Appl Inf. 2012;14(1):58–66.
17. Hudgins B, Parker P, Scott RN. A new strategy for multifunction myoelectric control. IEEE Trans Biomed Eng. 1993;40:82–94.
18. Chowdhury RH, Reaz MBI, Ali MABM, Bakar AAA, Chellappan K, Chang TG. Surface electromyography signal processing and classification techniques. Sensors (Basel). 2013;13:12431–66.
19. Farina D, Merletti R, Indino B, Graven-Nielsen T. Surface EMG crosstalk evaluated from experimental recordings and simulated signals. Reflections on crosstalk interpretation, quantification and reduction. Methods Inf Med. 2004;43:30–5.
20. Andrade AO, Soares AB, Nasuto SJ, Kyberd PJ. EMG decomposition and artefact removal. In: Computational intelligence in electromyography analysis—a perspective on current applications and future challenges. IntechOpen; 2012.
21. Shobaki MM, Malik NA, Khan S, Nurashikin A, Haider S, Larbani S, et al. High quality acquisition of surface electromyography—conditioning circuit design. In: IOP conference series: materials science and engineering, vol. 53. 2013. p. 012027.
22. Agostini V, Knaflitz M. An algorithm for the estimation of the signal-to-noise ratio in surface myoelectric signals generated during cyclic movements. IEEE Trans Biomed Eng. 2012;59:219–25.
23. Supuk TG, Skelin AK, Cic M. Design, development and testing of a low-cost sEMG system and its use in recording muscle activity in human gait. Sensors (Basel). 2014;14:8235–58.
24. Imtiaz U, Bartolomeo L, Lin Z, Sessa S, Ishii H, Saito K, et al. Design of a wireless miniature low cost EMG sensor using gold plated dry electrodes for biomechanics research. In: 2013 IEEE international conference on mechatronics and automation. 2013. p. 957–62.
25. Drost G, Stegeman DF, van Engelen BGM, Zwarts MJ. Clinical applications of high-density surface EMG: a systematic review. J Electromyogr Kinesiol. 2006;16:586–602.
26. Farina D, Jiang N, Rehbaum H, Holobar A, Graimann B, Dietl H, et al. The extraction of neural information from the surface EMG for the control of upper-limb prostheses: emerging avenues and challenges. IEEE Trans Neural Syst Rehabil Eng. 2014;22:797–809.
27. Farrell TR, Weir RF. The optimal controller delay for myoelectric prostheses. IEEE Trans Neural Syst Rehabil Eng. 2007;15:111–8.
28. Milosevic B, Benatti S, Farella E. Design challenges for wearable EMG applications. In: Design, Automation Test in Europe Conference Exhibition (DATE), 2017; 2017. p. 1432–7.
29. Electrode|Electrodes|Myo Control Elements|Myo Hands and Components|Upper Limb Prosthetics| Prosthetics|Ottobock US Healthcare [Internet]. [cited 2018 Dec 4]. https://professionals.ottobockus.com/Prosthetics/Upper-Limb-Prosthetics/Myo-Hands-and-Components/Myo-Control-Elements/Electrodes/Electrode/p/13E200~560.
30. Pizzolato S, Tagliapietra L, Cognolato M, Reggiani M, Müller H, Atzori M. Comparison of six electromyography acquisition setups on hand movement classification tasks. PLoS ONE. 2017;12:e0186132.
31. MyoWare Muscle Sensor—SEN-13723—SparkFun Electronics [Internet]. [cited 2019 Jan 28]. https://www.sparkfun.com/products/13723.
32. Gerdle B, Karlsson S, Day S, Djupsjöbacka M. Acquisition, processing and analysis of the surface electromyogram. In: Windhorst U, Johansson H, editors. Modern techniques in neuroscience research. Berlin: Springer; 1999. p. 705–55. https://doi.org/10.1007/978-3-642-58552-4_26.
33. Wang J, Tang L, Bronlund JE. Surface EMG signal amplification and filtering. Int J Comput Appl. 2013;82:15–22.
34. Rice DA, Venkatachalam V, Wegmann MJ. A simple envelope detector. IEEE Trans Instrum Meas. 1988;37:223–6.
35. Patla AE. Some characteristics of EMG patterns during locomotion: implications for the locomotor control process. J Mot Behav. 1985;17:443–61.
36. Medved V, Tomkovic S. Locomotion diagnostics: some neuromuscular and robotic aspects. IEEE Eng Med Biol Mag. 1991;10:23–8.
37. D'Alessio T, Conforto S. Extraction of the envelope from surface EMG signals. IEEE Eng Med Biol Mag. 2001;20:55–61.
38. Balbinot A, Favieiro G. A neuro-fuzzy system for characterization of arm movements. Sensors (Basel). 2013;13:2613–30.
39. FSR Integration Guide—Interlink Electronics|DigiKey [Internet]. [cited 2019 Jun 15]. https://www.digikey.com/en/pdf/i/interlink-electronics/interlink-electronics-fsr-force-sensing-resistors-integration-guide.
40. Konrad P. A practical introduction to kinesiological electromyography. 61.
41. Grimnes S. Impedance measurement of individual skin surface electrodes. Med Biol Eng Comput. 1983;21:750–5.
42. Sinderby C, Lindström L, Grassino AE. Automatic assessment of electromyogram quality. J Appl Physiol. 1995;79:1803–15.
43. Thuau D, Abbas M, Chambon S, Tardy P, Wantz G, Poulin P, et al. Sensitivity enhancement of a flexible MEMS strain sensor by a field effect transistor in an all organic approach. Org Electron. 2014;15:3096–100.
44. Rodrigues DMC, Lopes RN, Franco MAR, Werneck MM, Allil RCSB. Sensitivity analysis of different shapes of a plastic optical fiber-based immunosensor for *Escherichia coli*: simulation and experimental results. Sensors. 2017;17:2944.
45. Greene EJ, Lo PH. Method for measuring RF pulse rise time, fall time and pulse width. United States patent US 5,805,460. 1998.
46. Englehart K, Hudgin B, Parker PA. A wavelet-based continuous classification scheme for multifunction myoelectric control. IEEE Trans Biomed Eng. 2001;48:302–11.
47. Kargov A, Pylatiuk C, Martin J, Schulz S, Döderlein L. A comparison of the grip force distribution in natural hands and in prosthetic hands. Disabil Rehabil. 2004;26:705–11.
48. Geethanjali P. Myoelectric control of prosthetic hands: state-of-the-art review. Med Devices (Auckl). 2016;9:247–55.
49. Belter JT, Segil JL, Dollar AM, Weir RF. Mechanical design and performance specifications of anthropomorphic prosthetic hands: a review. J Rehabil Res Dev. 2013;50:599.